

# Geometry of subduction and depth of the seismogenic zone in the Guerrero gap, Mexico

Gerardo Suárez\*, Tony Monfret\*†, Gerard Wittlinger‡ & Christian David‡

\* Instituto de Geofísica, Universidad Nacional Autónoma de México, México DF 04510, Mexico

† Mission ORSTOM-Mexique, Homero 1804-1002 México DF 11510, Mexico

‡ Institut de Physique du Globe, 5 rue René Descartes, Strasbourg 68084 Cedex, France

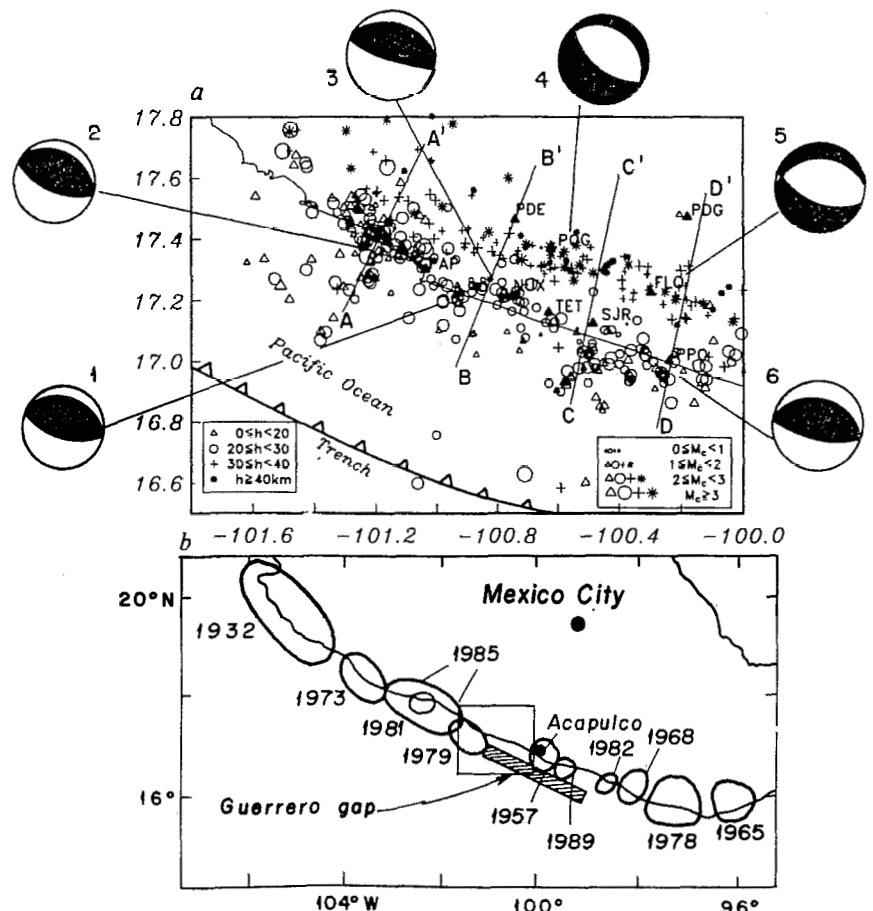
THE western coast of Guerrero in southern Mexico has been identified as a seismic gap on the Middle American Trench in which no large earthquakes have occurred at least since 1908. It has been suggested that the seismic energy accumulated since 1908 will eventually be released by a large earthquake. A permanent seismic network was installed to monitor the seismicity of this mature seismic gap and to understand the geometry of the subducted slab beneath this region. The seismicity defines an unusual distribution along two bands of seismic activity parallel to the coast. The resulting geometry of the subduction zone shows that the Cocos plate dips at a shallow angle beneath the North American plate to a depth of ~40 km; from there the subducted slab is bent upward, following a subhorizontal trajectory extending inland at a depth of ~50 km. This plate geometry is reminiscent of that found in Peru and central Argentina, two other regions where a young oceanic plate is being subducted. In Mexico, however, the slab underplates an overriding plate which is only half as thick as that observed in South America. A possible oceanic origin of the allochthonous terranes comprising southern Mexico may explain the presence of the anomalously thin lithosphere in this region.

The Guerrero gap in southern Mexico is perhaps one of the more clearly identified seismic gaps in the circum-Pacific belt<sup>1-3</sup>. It lies immediately south of the rupture area of the 1985 Michoacan earthquake<sup>4,5</sup> (Fig. 1). A telemetered, nine-station seismic network northwest of Acapulco (Fig. 1) records daily an average of four to five earthquakes, with coda-wave magnitude ( $M_c$ ) in the range 1-4, which are located using the program HYP071 (ref. 6) and a velocity model reported for this area<sup>7</sup>. The results presented here include events recorded during a three-month temporary experiment performed in 1986 and earthquakes located from August 1987 to December 1988 by the permanent network.

The distribution of seismicity shows an unusual disposition along two bands of activity (Fig. 1). The coastal band of seismicity is ~35 km wide and shows hypocentres with focal depths of between 10 and 25 km. The second zone of seismicity lies farther inland and is clearly separated from the coastal activity, showing focal depths of between 32 and 42 km. The absence of earthquakes between these two seismic bands is more evident where the station coverage is best. Also, practically no seismic activity is located between the coastal seismic zone and the trench (Fig. 1). Although this area is outside the network, the absence of seismic activity here is not due to its distance to the seismic instruments on land; small earthquakes ( $0 < M_c < 1$ ) are routinely located along the coast at equivalent distances from the centre of the network. This low level of near-trench seismicity appears where saturated sediments may have a dominant role in the mechanical behaviour of the plate interface.

In cross-section, the hypocentral distribution reflects the subduction of the Cocos plate beneath Mexico (Fig. 2). The void of seismicity between depths of 25 and 32 km, separating the two parallel seismic zones, is clearly visible on cross-sections where the accuracy of the locations is better (BB', CC' and DD'). The apparent absence of this void in section AA' probably reflects poor hypocentral control of earthquakes located outside

FIG. 1 a, Map showing the location of stations of the Guerrero seismic network (solid triangles) and of the selected epicentres. Cross-sections are shown in Fig. 2. Composite fault-plane solutions are in lower-hemispheric projection; solid quadrants indicate compressional first motions. b, Location of the Guerrero gap relative to the rupture areas of previous large earthquakes in the region. Station coordinates: PDE, 17.46°N, 100.74°W; TET, 17.16°N, 100.63°W; NUX, 17.21°N, 100.75°W; PAP, 17.30°N, 101.04°W; POP, 17.02°N, 100.24°W; FLO, 17.22°N, 100.39°W; POG, 17.37°N, 100.62°W; PDG, 17.47°N, 100.18°W; SJR, 17.14°N, 100.47°W.



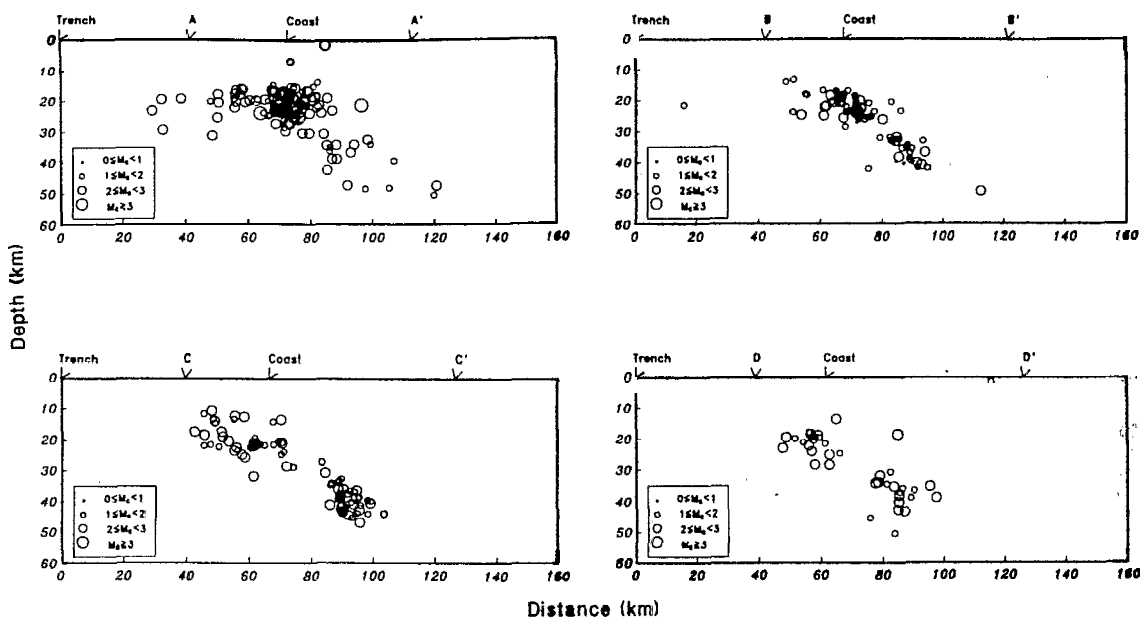
15 MAI 1991

ORSTOM Fonds Documentaire

N° : 31-928 ex 1

Cote : B p 34 M

FIG. 2 Cross-sections of the seismicity (open circles) shown on Fig. 1. Size of symbols indicate magnitude of hypocentres. Notice the two distinct seismic clusters in the three cross-sections made within the seismic network (BB', CC' and DD').



of the network. Notice also that the overriding plate is virtually aseismic (Fig. 2). Composite fault-plane solutions of the coastal earthquakes show shallow-thrust faulting dipping to the northeast, reflecting the relative motion of the Cocos and North American plates (Figs 1 and 3). On the other hand, the deeper seismic zone shows predominantly normal faulting with tensional axes almost horizontal and oriented in the direction of relative plate motion (Figs 1 and 3).

No microseismicity was located inland of the second seismic band. Because of this, the trajectory of the subducted slab farther inland can not be determined only from the microearthquakes located by the network. Nevertheless, some large events occurring inland have been studied using teleseismic data, such as the Tlapehuala event of 6 June 1964 ( $M_s = 6.7$ ). Its focal mechanism and hypocentral depth are well constrained using body-wave modelling<sup>8</sup>, indicating normal faulting with almost horizontal T-axis oriented NNE-SSW (Fig. 4) at a depth of 55 km, similar to that of other tensional earthquakes within the subducted slab in central Mexico<sup>9-13</sup>. Another earthquake on 2 July 1968 also shows (ref. 14) normal faulting at a depth of 45 km<sup>14</sup> in the region where no seismicity has been recorded by the network. The geometry of the slab is inferred by projecting the hypocentre of these two earthquakes onto a cross-section together with the microseismic data (Fig. 4).

The data show that the Cocos plate subducts beneath the North American plate at a shallow angle which steepens progressively to  $\sim 12^\circ$ . The maximum depth of strong seismogenic plate contact is 25 km. Beneath this depth the subducted slab bends sharply, following a quasi-horizontal trajectory underplating southern Mexico for at least 150 km (Fig. 4). The narrow coastal seismicity reflects the relative motion of the Cocos and North American plates, whereas the tensional earthquakes located deeper and farther inland seem to reflect flexural stresses induced by the sharp bend in the slab. The morphology of the slab to the north of the flat portion is still not known (Fig. 4). Probably the slab steepens north of this region, reaching a depth of  $\sim 100$  km beneath the volcanic belt, as observed in most subduction zones<sup>15</sup>. The apparent buoyancy of the slab in central Mexico may be due to the young age of the Cocos plate. In southeastern Mexico and Central America, where the Cocos plate is older<sup>16</sup>, the slab dip becomes steeper ( $30^\circ$ ) with no evidence of a horizontal segment<sup>10-12</sup>.

The flexure of the subducted slab near the coast may explain also the presence of great, lithospheric tensional earthquakes occurring in Mexico immediately downdip of the megathrust plate contact. The 15 January 1931 event in Oaxaca ( $M_w = 8.0$ )<sup>13</sup>, and probably the great earthquake of 19 June 1858 in northern

Michoacan ( $M_w \approx 8.0$ ), are difficult to explain by the purported gravitational pull of a slab that is subhorizontal and shallower than  $\sim 100$  km in central Mexico<sup>11,12</sup>. Their origin is perhaps better explained by flexural stresses present in the contorted slab.

This bend in the slab at a depth of  $\sim 30$  km apparently limits

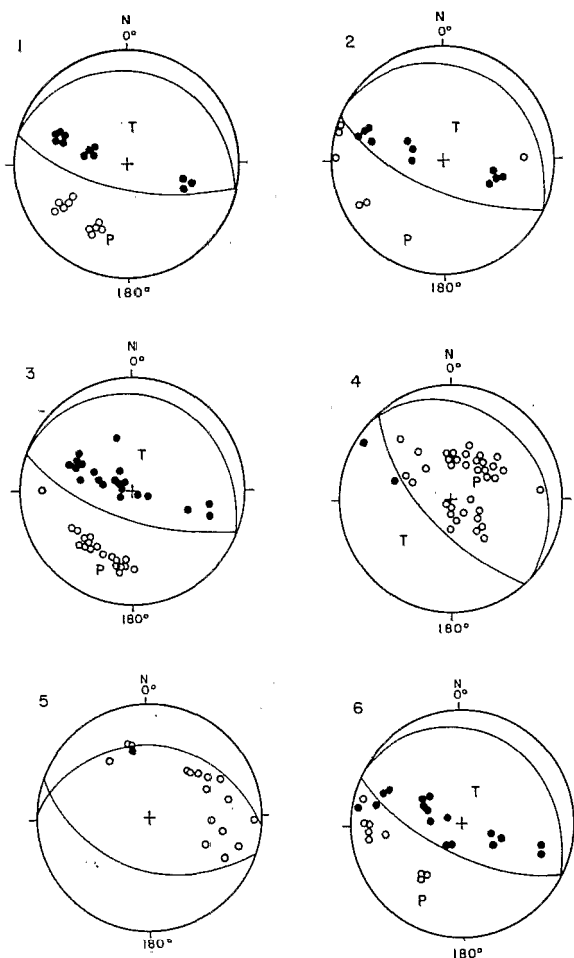


FIG. 3 Composite focal mechanisms of the earthquakes shown on Fig. 1. Solid circles indicate compressional first motions; smaller symbols are indicative of nodal arrivals. The letters P and T indicate axes of maximum and minimum compression respectively. Projection is on a lower-hemisphere stereonet.

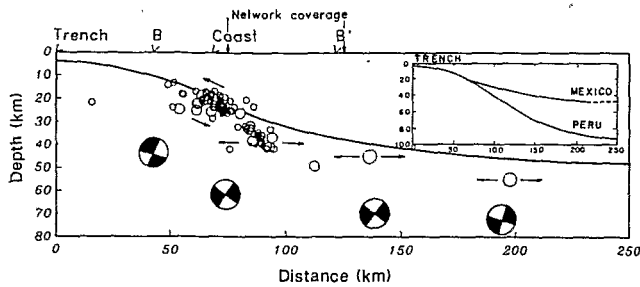


FIG. 4 Geometry of the subducted slab beneath southern Mexico. Seismicity corresponds to that of cross-section CC' on Figs 1 and 2. Focal mechanisms of microearthquakes and of teleseismic events<sup>8,14</sup> are shown on side-looking, lower-hemisphere projection. Dark quadrants indicate compressional first motions. Arrows indicate approximate projected orientation of the T-axes. Inset shows comparison between subduction zones in central Peru<sup>22,23</sup> and southern Mexico. Notice the continental lithosphere in Peru is twice as thick as that of Mexico.

the downdip extent of the seismogenic zone, explaining the unusually narrow megathrust plate contact found in the Mexican subduction zone; a fact corroborated by aftershock studies performed after large subduction earthquakes in Mexico<sup>4,5,7,17-19</sup>, which show that the rupture areas of interplate events in this region are consistently shallower than 20 km. This relatively narrow seismogenic interface in Mexico may explain why the Middle American arc, where young oceanic lithosphere is being subducted at a fast rate ( $\sim 6.5 \text{ cm yr}^{-1}$ ), does not have the large contact zone that results in major earthquakes ( $M_w > 9.0$ ) like those of 1960 in Chile or 1964 in Alaska. The seismogenic zone in Guerrero is as narrow as the 1985 Michoacan rupture. Thus, the length of the northwestern Guerrero gap would result in an earthquake of the same magnitude as the 1985 event ( $M_w = 8.1$ ). If the rupture propagates south of Acapulco, the magnitude could be as high as 8.4.

The plate geometry in Guerrero is reminiscent of that observed in central Peru<sup>20-23</sup> and Argentina<sup>12,20,24</sup>, where the Nazca plate lies subhorizontally, underplating the South American plate. central Peru, Argentina, and central Mexico are apparently the only three subduction zones that exhibit a horizontal slab beneath the upper continental plate. However, the main difference between the subduction in Mexico and those of South America is the lithospheric thickness of the overriding plate. Locally recorded microearthquakes<sup>21-23,25</sup> and accurate depth determinations of teleseismic events<sup>22,24</sup>, show the horizontal seismic zone beneath central Peru and Argentina lies at an average depth of 100 km, which corresponds to a lithospheric thickness of  $\sim 90$  km. In contrast, the average lithospheric thickness in southern Mexico is only  $\sim 45$  km (Fig. 4).

This thin lithosphere in southern Mexico is more similar to that of an oceanic plate<sup>26</sup> than to the thicker continental lithosphere<sup>27</sup> expected in this region. This is probably explained by the fact that southern Mexico was formed by the accretion of allochthonous terranes onto the continent since the Palaeozoic<sup>28-31</sup>. The thin lithosphere underlying these allochthonous terranes suggests they may be oceanic in nature. Otherwise, the lithosphere in southern Mexico could be originally continental and later thinned by an extensional phase of deformation when swarms of mafic dykes were intruded<sup>29,32</sup>. In any case, the young and presumably buoyant subducted slab seems likely to follow the lower topography of this thin overriding plate. □

Received 16 October 1989; accepted 9 March 1990.

1. Kelleher, J., Sykes, L. & Oliver, J. *J. geophys. Res.* **78**, 2547-2585 (1973).
2. McNally, K. & Minster, J. B. *J. geophys. Res.* **86**, 4949-4959 (1981).
3. Nishenko, S. & Singh, S. K. *Bull. seism. Soc. Am.* **77**, 2095-2114 (1987).
4. UNAM Seismology Group *Geophys. Res. Lett.* **13**, 573-576 (1986).

5. Stolte, C. et al. *Geophys. Res. Lett.* **13**, 577-580 (1986).
6. Lee, W. H. K. & Lahr, J. C. *U.S. Geol. Surv., Open File Report* 75-311 (1975).
7. Valdes, C., Meyer, R. P., Zúñiga, R., Havskov, J. & Singh, S. K. *J. geophys. Res.* **87**, 8519-8527 (1982).
8. González-Ruiz, J. thesis, Univ. of California, Santa Cruz (1986).
9. Jiménez, Z. & Ponce, L. *Geofis. Int.* **17**, 379-386 (1979).
10. Nixon, G. T. *Bull. geol. Soc. Am.* **93**, 514-523 (1982).
11. Burbach, G. V., Frohlich, C., Pennington, W. D. & Matsumoto, T. *J. geophys. Res.* **89**, 7719-7735 (1984).
12. Bevis, M. & Isacks, B. *J. geophys. Res.* **89**, 6153-6170 (1984).
13. Singh, S. K., Suárez, G. & Domínguez, T. *Nature* **317**, 56-58 (1985).
14. Molnar, P. & Sykes, L. R. *Bull. geol. Soc. Am.* **80**, 1639-1684 (1969).
15. Isacks, B. & Barazangi, M. *Maurice Ewing Series 1*, *Am. Geophys. Union*, 99-114 (1977).
16. Couch, R. & Woodcock, S. *J. geophys. Res.* **86**, 1829-1840 (1981).
17. Ponce, L., McNally, K. C., González, J., Del Castillo, L. & Chael, E. *Geofis. Int.* **17**, 267-280 (1979).
18. Singh, S. K. et al. *Science* **207**, 1211-1213 (1980).
19. Havskov, J., Singh, S. K., Nava, E., Domínguez, T. & Rodríguez, M. *Bull. seism. Soc. Am.* **73**, 449-458 (1983).
20. Barazangi, M. & Isacks, B. *Geophys. J. R. astr. Soc.* **57**, 537-555 (1979).
21. Grange, F. et al. *J. geophys. Res.* **89**, 6139-6152 (1984).
22. Hasegawa, A. & Sacks, I. S. *J. geophys. Res.* **86**, 4971-4980 (1981).
23. Suárez, G. et al. *Geophys. J.* (in the press).
24. Araujo, M. & Suárez, G. *J. geophys. Res.* (submitted).
25. Grange, F. et al. *Geophys. Res. Lett.* **11**, 38-41 (1982).
26. Forsyth, D. *Geophys. J. R. astr. Soc.* **43**, 103-162 (1975).
27. Press, F. *J. geophys. Res.* **75**, 6575-6581 (1970).
28. Campa, M. F. & Coney, P. *Can. J. Earth Sci.* **26**, 1040-1051 (1983).
29. Ortega-Gutiérrez, F. *Geofis. Int.* **20**, 177-202 (1981).
30. Pantoja-Alor, J. & Estrada-Barraza, M. *Bol. Soc. geol. Mex.* **48**, 1-15 (1986).
31. Gastil, G., Krumeracher, D. & Jenschky, W. A. *Geol. Soc. Am. Map Chart Ser.*, M24, (1978).
32. Cserna, Z. *Bol.* **62**, Inst. Geol., Univ. Nac. Auton. Mex. (1965).

ACKNOWLEDGEMENTS. We thank G. Ball, J. A. Estrada, J. M. Holl, and S. Solis for technical support in building and maintaining the Guerrero seismic network, and F. Megard and R. Gaulon for their support. We also thank H. Lyon-Caen, F. Ortega, L. Ponce, E. Rosenblueth, J. Urrutia and R. Zúñiga for discussions. J. Domínguez and A. Araujo helped us read the seismic data. We acknowledge support from the Ministry of Foreign Affairs of France and the Mexican National Council of Science and Technology (CONACYT).

## Implications of a new acoustic target strength for abundance estimates of Antarctic krill

Inigo Everson\*, Jonathan L. Watkins\*, Douglas G. Bone\* & Kenneth G. Foote†

\* British Antarctic Survey, High Cross, Madingley Road, Cambridge CB3 0ET, UK

† Institute of Marine Research, PO Box 1870 Nordnes, 5024 Bergen, Norway

ANTARCTIC krill (*Euphausia superba*) is the dominant component of the diet of many whales, seals, birds, fish and squid, and their survival could be affected by a reduction in krill abundance due to fishing<sup>1</sup>. Commercial fishing takes nearly half a million tonnes of krill annually<sup>2</sup> and accurate estimates of abundance are needed for rational management of this resource. Indirect estimates of abundance based on predator consumption rates give a roughly estimated total annual production of several hundred million tonnes<sup>3</sup>. The life-span of krill is at least two and maybe five years, so the standing stock would need to be of at least the same magnitude as the annual production. But direct estimates of abundance using nets and acoustics have indicated biomass figures lower by an order of magnitude<sup>3</sup>. Acoustic estimates are sensitive to the scaling factor or target strength (TS) used to convert echo energy to absolute abundance. Previous published values for TS (ref. 4), when applied to survey data, gave estimates of krill abundance that were much too low to account for local bird and seal predation rates near South Georgia<sup>5</sup>, and were also lower than expected when compared with density estimates from net hauls<sup>6</sup>. We therefore sought to determine TS using direct measurements developed for fish studies<sup>7</sup>, and also by applying models developed for other crustacean zooplankton<sup>8</sup>. Our results show that krill TS is much lower than previously thought, and consequently that acoustic estimates of krill abundance are likely to have been gross underestimates.

The field study was undertaken in Stromness Harbour, South Georgia; a comprehensive description of the methodology is published elsewhere<sup>9</sup>. Mean TS values for groups of krill were